

Structure and elastic properties of $\text{Mg}(\text{OH})_2$ from density functional theory

Paweł T Jochym, Andrzej M Oleś, Krzysztof Parlinski, Jan Łażewski, Przemysław Piekarczyk and Małgorzata Sternik

Institute of Nuclear Physics, Polish Academy of Sciences, Radzikowskiego 152, PL-31342 Kraków, Poland

E-mail: Pawel.Jochym@ifj.edu.pl

Abstract. The structure, lattice dynamics and mechanical properties of the magnesium hydroxide have been investigated with static density functional theory calculations as well as *ab initio* molecular dynamics. The hypothesis of a superstructure existing in the lattice formed by the hydrogen atoms has been tested. The elastic constants of the material have been calculated with static deformations approach and are in fair agreement with the experimental data. The hydrogen subsystem structure exhibits signs of disordered behaviour while maintaining correlations between angular positions of neighbouring atoms. We establish that the essential angular correlations between hydrogen positions are maintained to the temperature of at least 150 K and show that they are well described by a physically motivated probabilistic model. The rotational degree of freedom appears to be decoupled from the lattice directions above 30K.

PACS numbers: 62.20.dq, 65.40.-b, 71.15.Mb

Submitted to: *J. Phys.: Condens. Matter*

1. Introduction

The magnesium hydroxide — $\text{Mg}(\text{OH})_2$ — is a very simple mineral, called brucite, often regarded as a good example of a material with structurally bound OH group. The large number of known silicate phases with such structurally bound OH units [1, 2] motivates high interest in the role played by the OH groups and the physical properties induced by them of this type of crystals in the Earth interior. Brucite was a subject of numerous experimental [3, 4, 5, 6, 9, 7, 8] and theoretical [9, 10, 11, 12] studies in the past. Despite its simple structure, its physical properties remain still unexplored — in fact even its crystallographic symmetry has not been fully established [13], although the question about its structure has been addressed several times in the past [9, 10, 11, 12].

The crystal lattice of the magnesium hydroxide is a simple, layered, hexagonal structure with layers of magnesium interlaced with layers of hydroxyl groups. This basic structure was firmly established long time ago [14] as having $P\bar{3}m1$ symmetry with O-H bond aligned on a three-fold axis (see figure 1). Further research [15] showed unexpectedly high thermal displacements of hydrogen atoms. The models proposed

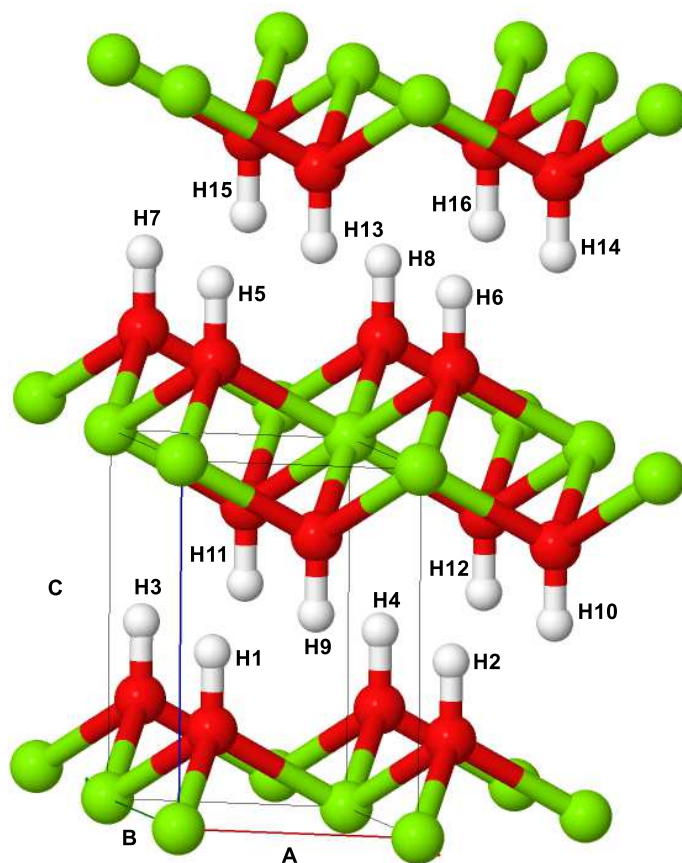


Figure 1. Schematic view of the structure of a brucite crystal. The figure shows $2 \times 2 \times 2$ supercell used in the numerical calculations, while the primitive unit cell is indicated by the (smaller) grey box. Dark grey (red) and light grey (green) balls show the positions of O and Mg atoms, respectively. The labels of the hydrogen atoms shown by light (white) balls are used to analyse their structural correlations in the text.

until now [9, 7, 13, 16, 17, 18] deal with temporary and spatially averaged positions of the hydrogen subsystem and suggest that the hydrogen atoms are in fact displaced from the high symmetry points on the three-fold axis to form a new lattice with $P\bar{3}$ symmetry and averaged $1/3$ occupancy of three equivalent $6i$ Wyckoff positions $(x, 2x, z)$, with either $x > 1/3$ (so called XGT arrangement) [9, 7, 13, 17, 18], or $x < 1/3$ (so called XLT arrangement) as proposed by Megaw [16]. The schematic placement of atoms in this larger unit cell is presented in figure 2. The case for the XGT arrangement is further strengthened by the neutron diffraction experiment of Desgranges *et al.* [19] indicating that protons are displaced into XGT positions even

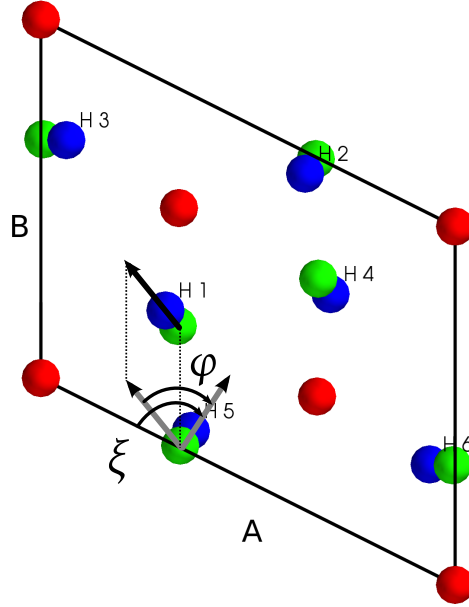


Figure 2. Schematic atomic positions in the $P\bar{3}$ structure of a brucite crystal. The primitive unit cell is the size of $\sqrt{3} \times \sqrt{3} \times 1$ of the unit cell of the $P\bar{3}m$ structure shown in figure 1. The corners are occupied by Mg atoms (grey, red balls), and each H atom (dark, blue ball) is accompanied by an O atom (light, green ball). The labels of the hydrogen atoms are used later in the text to investigate their spatial correlations. The angles shown here for h5 atom represent its relative angular coordinate φ with respect to the reference atom H1, and an absolute angular coordinate ξ .

at ambient pressure.

All the above models could reflect true structure of the brucite crystal but due to the performed spatial and temporal averaging of the structure they may miss the dynamical aspect. In the present paper we deal with this aspect of the magnesium hydroxide structure. Firstly, we are going to show results of the static, elastic constants calculations for the crystal followed by the results of the density functional theory (DFT) molecular dynamics (MD) calculations of the brucite crystal's structural properties. Secondly, we analyse the dynamical aspects of the structure and demonstrate that the hydrogen atoms are not frozen in their equilibrium positions but fluctuate strongly, displaying some unexpected dynamical structure characterized by long range spatial correlations.

The paper is organized as follows. In section 2 the calculation method is presented. It serves to derive elastic constants of the magnesium hydroxide which are reported and compared with available experimental values in section 3. Next, in section 4.1, we investigate the dynamical model of the hydrogen structure, showing that the short-range correlations persist and relative hydrogen positions may be described by a simple probabilistic model presented in section 4.2). The paper is concluded in section 5.

Table 1. Elastic constants for increasing pressure P (all quantities in GPa) obtained for the high symmetry ($P\bar{3}m1$) unit cell of the magnesium hydroxide.

P	C_{11}	C_{33}	C_{12}	C_{13}	C_{44}
1.4	126.6	534.0	112.7	39.6	61.8
2.1	131.2	541.8	116.1	40.8	64.3
2.7	135.5	549.5	118.9	41.5	66.9

2. Calculation setup

We have performed all calculations of the structure and elastic properties of the magnesium hydroxide using VASP,[20] a DFT based code employing the generalized gradient approximation (GGA) [21] with Perdew, Burke, and Ernzerhof (PBE) [22] projector augmented-wave (PAW) pseudopotentials [23, 21]. The reciprocal space integration has been carried out over the set of special points generated according to the Monkhorst-Pack scheme [24].

The static calculations have been carried out with a single hexagonal unit cell shown by a grey box in figure 1, a $\sqrt{3} \times \sqrt{3} \times 1$ supercell (figure 2) and reciprocal space sampling based on $2 \times 2 \times 2$ lattice. The calculation of elastic constants has used the standard finite deformation method described in detail in the previous publications [25, 26]. We have applied displacements between $\{0.1\%; 0.1^\circ\}$ and $\{1\%; 1^\circ\}$ for the lattice vector lengths and angles, respectively.

The schematic structure of the crystal in the $2 \times 2 \times 2$ supercell is presented in figure 1 together with the adopted numbering scheme of hydrogen atoms used later in section 4 in the analysis of inter-atomic correlations. The MD calculations have been conducted with both $\sqrt{3} \times \sqrt{3} \times 1$ and $2 \times 2 \times 2$ unit cells with the standard energy cut-off, $E_{\text{cut}}=400\text{eV}$, determined by the used pseudopotentials. We have performed several 3 ps runs with 1-1.5 fs time step for temperatures ranging from 10 K to 150 K in micro-canonical ensemble (constant total energy) with at least 10 ps thermalization runs carried out with Nosé thermostat technique [27]. The trajectories collected from the MD runs were further analysed to extract positional correlations using the computer code developed for this purpose.

To check the influence of the supercell size on obtained results we have calculated — using standard direct method [28, 29] — the force constants matrix and full lattice dynamics for the larger ($3 \times 3 \times 3$) system as well as the smaller one used in the MD calculations ($2 \times 2 \times 2$). The obtained exponential dependence of force constants on distance shows that the inclusion of the next layer of unit cells in the system contributes less than 1/1000 of the overall interaction between atoms in the system. Furthermore, the dispersion curves and phonon density of states spectra, calculated for both ($2 \times 2 \times 2$ and $3 \times 3 \times 3$) systems, display no significant difference, which means that the inclusion of the additional layer of unit cells does not modify the lattice dynamics of the system in any significant way and the conclusions concerning lattice vibrations drawn from the present calculations are robust.

3. Elastic constants

We have completed a series of static, elastic constants calculations using various sizes and symmetries of the unit cells and atomic positions: high-symmetry ($P\bar{3}m1$)

Table 2. Elastic constants of the magnesium hydroxide for increasing pressure P (all quantities in GPa), measured by Jiang *et al.* [30] with Brillouin scattering.

P	C_{11}	C_{33}	C_{12}	C_{13}	C_{44}
10^{-4}	159.0(16)	49.5(7)	43.3(17)	11.1(25)	22.8(4)
1.1(1)	164.1(10)	59.2(7)	45.5(8)	12.3(8)	25.2(3)
2.1(1)	169.3(9)	73.2(7)	46.2(8)	16.6(7)	28.9(3)
3.5(1)	179.6(10)	94.0(8)	52.0(9)	22.1(8)	33.4(3)
4.8(1)	184.3(8)	110.0(6)	53.1(6)	28.2(5)	36.8(3)

Table 3. Elastic constants for increasing pressure P (all quantities in GPa) obtained for the low symmetry ($P\bar{3}$) unit cell of the magnesium hydroxide.

P	C_{11}	C_{33}	C_{12}	C_{13}	C_{44}
0.01	130.6	48.5	70.3	10.0	20.4
0.96	133.5	51.9	67.8	9.8	24.2
2.0	143.4	82.6	73.4	17.7	29.3
3.0	150.0	93.5	76.3	15.7	32.9
4.0	153.9	104.2	76.1	22.1	36.6

experimental unit cell [14], low-symmetry ($P\bar{3}$) $\sqrt{3} \times \sqrt{3} \times 1$ supercell, both with standard (1%) and small deformations (0.1%). In general, some results presented in table 1 for the high-symmetry unit cell show fairly good agreement with experimental data [30], but others exhibit certain peculiarities which motivated our further investigation. While the obtained values of C_{11} are rather close to experimental ones, the calculated elastic constants C_{12} , C_{13} and C_{44} are systematically about twice higher than the experimental values (table 2). The largest difference close to one order of magnitude was obtained for C_{33} at $P \simeq 1$ GPa.

During calculations we have observed that the system shows large sensitivity of elastic constants to external stress applied to the unit cell. In some cases non-hydrostatic stress of approximately 1-2 GPa induced twofold change in C_{33} and C_{13} constants.

The discrepancy between theoretical and experimental values of elastic constants can be partially resolved by careful relaxation of the internal degrees of freedom of the system in the deformed state. The standard procedure calls for cell deformation while keeping the same fractional positions of atoms followed by the internal degrees of freedom relaxation. Since the hydrogen atoms start at high symmetry positions on the three-fold axis the straight-forward minimization procedure keeps this symmetry. Only after lifting this symmetry constraint, the true ground state obtained after deformation (with lower total energy) could be reached. The elastic constants obtained following this procedure become fairly close to the results of Brillouin scattering experiment summarized in table 2. As a result of this relaxation the hydrogen atoms are displaced from their starting high-symmetry positions $(\frac{1}{3}, \frac{2}{3}, z)$ and $(\frac{2}{3}, \frac{1}{3}, 1 - z)$.

Prompted by the above anomalies and concepts presented in the published research on the structure of $Mg(OH)_2$, we have calculated the same properties for the larger $\sqrt{3} \times \sqrt{3} \times 1$ unit cell with $P\bar{3}$ symmetry and hydrogen atoms displaced into XGT positions as suggested recently by Mookhejee and Stixrude [13]. This suggestion agrees also with the earlier results in the literature [9, 7, 17, 18]. Indeed, the values obtained

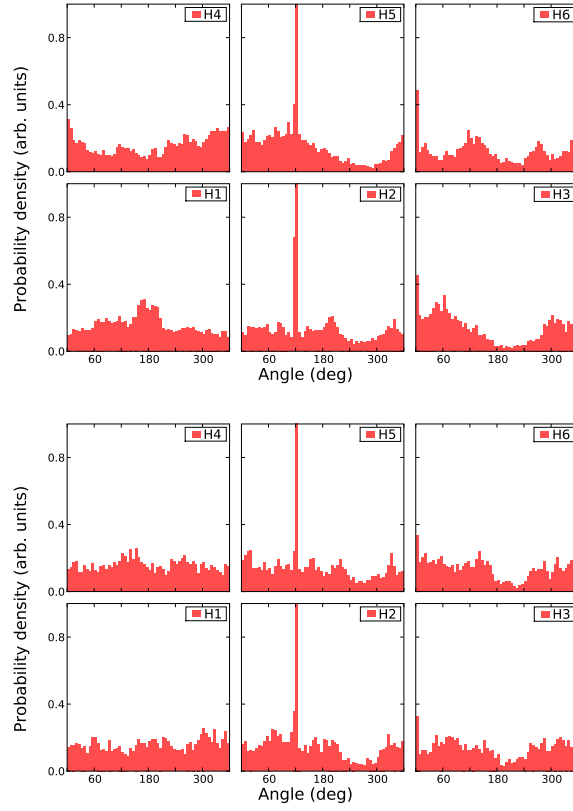


Figure 3. Absolute angular hydrogen distribution in $P\bar{3}$ unit cell. Top panels show results obtained from MD run at 244 K, and bottom ones at 46 K. The maxima at angle $\varphi \simeq 120^\circ$ obtained for H2 (H5) atoms are 2.05 and 1.2 (1.2 and 1.57) at high and low temperature, respectively. Positions of hydrogen atoms with labels H1,H2,...,H6 are shown in figure 1.

for this phase and presented in table 3 show much better agreement with experiment (table 2). We have also observed considerably weaker sensitivity of calculated values to the external stress applied to the system.

Moreover, during optimization of the magnesium hydroxide structure, we have observed that positions of hydrogen atoms around the three-fold axis are not very well constrained in the system, i.e., they probably move in a very shallow potential well. This observation is in concordance with previous experimental evidence [15]. It suggests that the structure of the magnesium hydroxide crystal may be more complicated than it is currently accepted.

4. Dynamical structure

4.1. Correlations between hydrogen positions

In order to explore further the issue of dynamical hydrogen structure in the magnesium hydroxide, we have used the DFT-based MD technique. The first calculation setup

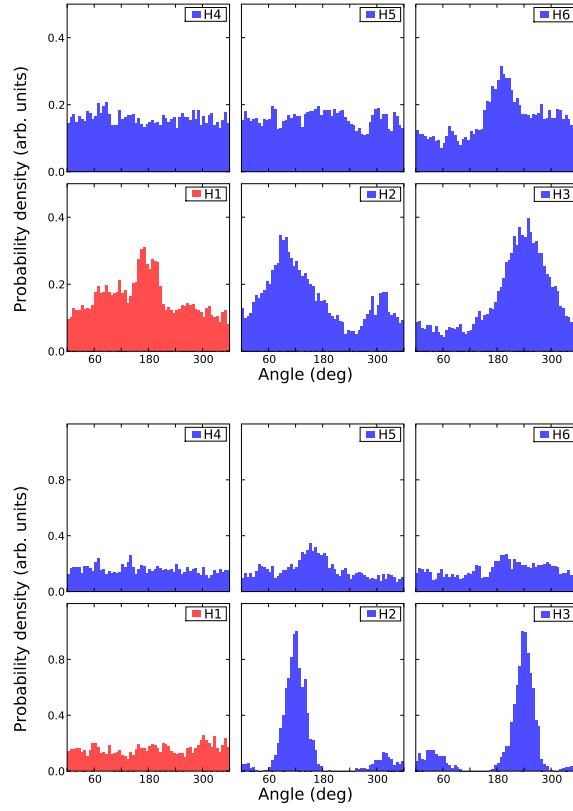


Figure 4. Relative angular hydrogen distribution in $P\bar{3}$ unit cell. The H_1 box shows absolute angular distribution of the H_1 atom. Top panels show results obtained from the MD run at 244 K, and bottom ones at 46 K. Positions of hydrogen atoms with labels H_1, H_2, \dots, H_6 are shown in figure 1.

used the $\sqrt{3} \times \sqrt{3} \times 1$, $P\bar{3}$ unit cell proposed by Mookherjee and Stixrude [13]. The data have been collected from measurement runs of 3 ps length each preceded by at least 10 ps thermalization run, for several temperatures between 15 K and 250 K.

The examination of the MD trajectories shows large amplitudes of hydrogen movements even for runs performed at low temperature. This result corresponds to large thermal displacements observed in the experiment [15]. On the one hand, some experimental results [19], showing clear symmetry of the hydrogen locations, may be seen as contradicting such observation, while on the other hand, correlations between the hydrogen movements could explain this discrepancy.

To resolve this dilemma we have developed a method to quantify angular correlations of hydrogen atoms. We extracted the correlation between positions of hydrogen atoms with respect to each other as well as with respect to the fixed reference crystal lattice. The results are presented in figure 3 for absolute hydrogen angular distribution and in figure 4 for relative hydrogen angular correlations. All these runs have been performed in the $\sqrt{3} \times \sqrt{3} \times 1$ unit cell. The angle φ is an angular position of the hydrogen atom around the three-fold axis, measured starting either from the direction of the crystal vector \vec{A} for absolute angular distributions (red histograms),

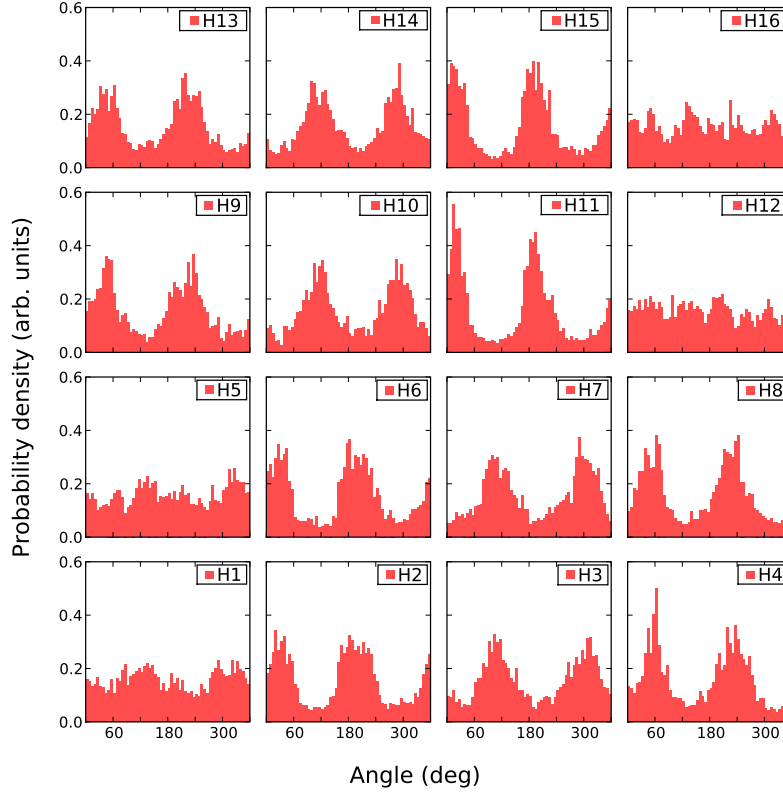


Figure 5. Absolute angular distribution of hydrogen atoms in the $2 \times 2 \times 2$ supercell. The results are obtained from a 6 ps MD run at 16 K. Positions of hydrogen atoms with labels H1,H2,...,H16 are shown in figure 1.

or from the direction selected by an arbitrary reference hydrogen atom (H_1 $[\frac{1}{3}, \frac{1}{3}, z_1]$ in our case) for relative angular distributions (blue histograms).

The high peaks seen in figure 3 suggest that there may be a lock-in of H2 and H5 hydrogen atom positions with respect to the crystal lattice. The lattice lock-in appears to be still present at 244 K (upper panel in figure 3) but we have to mention fairly strong and uniform background of other positions in the histogram. In fact, the most of the area in these histograms is *outside* the peaks. Thus, hydrogen atoms do not spend most of their time in the vicinity of their high symmetry positions. This means that, despite distinct peaks visible in the histograms, the angular positions of hydrogen atoms are *not* locked with respect to the crystal lattice orientation. Some of our results obtained for even lower temperatures ($T \approx 10$ K) indicate that the true lock-in with the crystal lattice may appear at or below $T = 15$ K — at this temperature we have observed Gaussian-shaped peaks and diminished background in the histograms (not shown). Unfortunately, due to the difficulties of the MD calculations performed at low temperature we were unable to collect enough evidence to confirm this indication.

The relative angular distribution results displayed in figure 4 show quite a different picture. On the one hand, there is a strong correlation, indicated by distinct peaks, of angular position between hydrogen atoms in the same layer (H_1 , H_2 , and H_3 positions

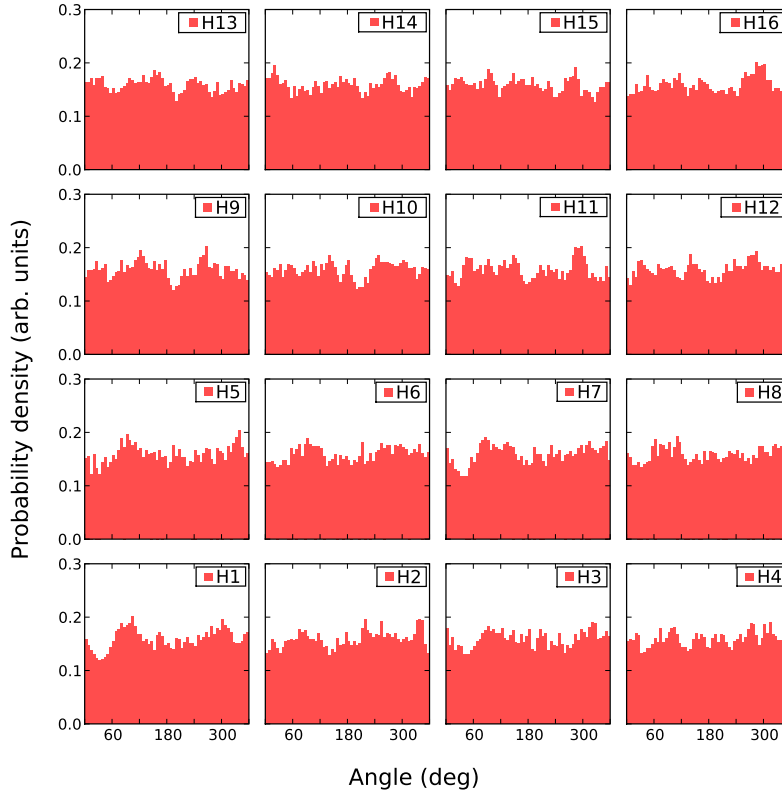


Figure 6. Absolute angular distribution of hydrogen atoms in the $2 \times 2 \times 2$ supercell. The result are obtained from a 39 ps MD run at 30 K. Positions of hydrogen atoms with labels H1,H2,...,H16 are shown in figure 1.

are as in figure 2). On the other hand, no visible correlations were found for the atoms in the next layer (H_4 , H_5 , and H_6). This means that the hydrogen atoms maintain relative orientations shown in figure 2, keeping their angular positions 120° apart — similar to the angular positions in the XGT/XLT structures mentioned in section 1 — but only if we consider atoms which belong to the same layer of the structure. On the contrary, the neighbouring layer positions appear only loosely coupled. These relations are maintained up to the highest temperature we have investigated (300 K), but broadening of the peaks observed at 244 K (upper panel of figure 4) suggests that the peaks may disappear at higher temperatures, as one would expect.

The above result supports, to some extent, the conclusions of the previous work on brucite crystal [9, 7, 13, 15, 17, 18, 19], except that the hydrogen-hydrogen correlations do not appear for all atoms, but only for neighbouring atoms in the same layer. Furthermore, the lock-in of hydrogen positions to the lattice is not well confirmed by the above results and probably vanishes above relatively low temperature of $T = 15$ K. These discrepancies motivated us to investigate the system further under less constraining conditions.

The results of the calculation performed for the larger $2 \times 2 \times 2$ unit cell at temperature $T = 16$ K are presented in figure 5. It is quite clear that the correlations

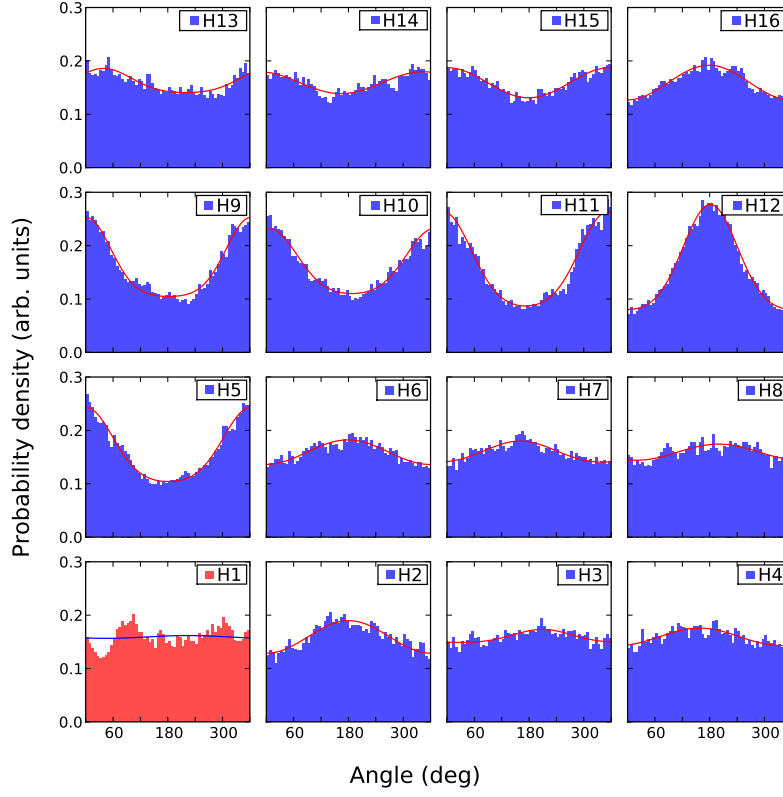


Figure 7. Relative angular distribution of hydrogen atoms in the $2 \times 2 \times 2$ supercell. The results are obtained from a 39 ps MD run at 30 K. Solid line shows the function $\mathcal{F}_\sigma(\varphi)$ given by equation (3) fitted to the data. Positions of hydrogen atoms with labels H1, H2, ..., H16 are shown in figure 1.

seen in the smaller unit cell are changed by the increase of the unit cell. We were unable to identify clearly any lock-in effect of the hydrogen positions with respect to the crystal lattice for the temperatures above 30 K (figure 6) but below this temperature the signal arising from locked-in hydrogen positions is distinct and robust (figure 5). We have performed the calculations for several temperatures in the low temperature regime and for different starting conditions and obtained the same result in all cases.

The relative angular correlations are still present when a larger unit cell is investigated, but they are also modified with respect to the ones found before with the smaller unit cell. The histograms seen in figure 6 show distributions of angular positions of hydrogen atoms relative to the crystal lattice and those shown in figure 7 — relative to an arbitrarily selected reference atom H₁, see figure 1. For the low temperature run (figure 5) we can easily identify obvious non-uniformities in the distribution of absolute angular positions of most hydrogen atoms. The absence of distinct peaks for some atoms may be interpreted as a result of the relatively short simulation time (6 ps) and insufficient statistics due to the difficulty of performing adequate sampling of configuration space at low temperatures. We have verified that the overall picture remains in fact similar for different runs, but individual peaks

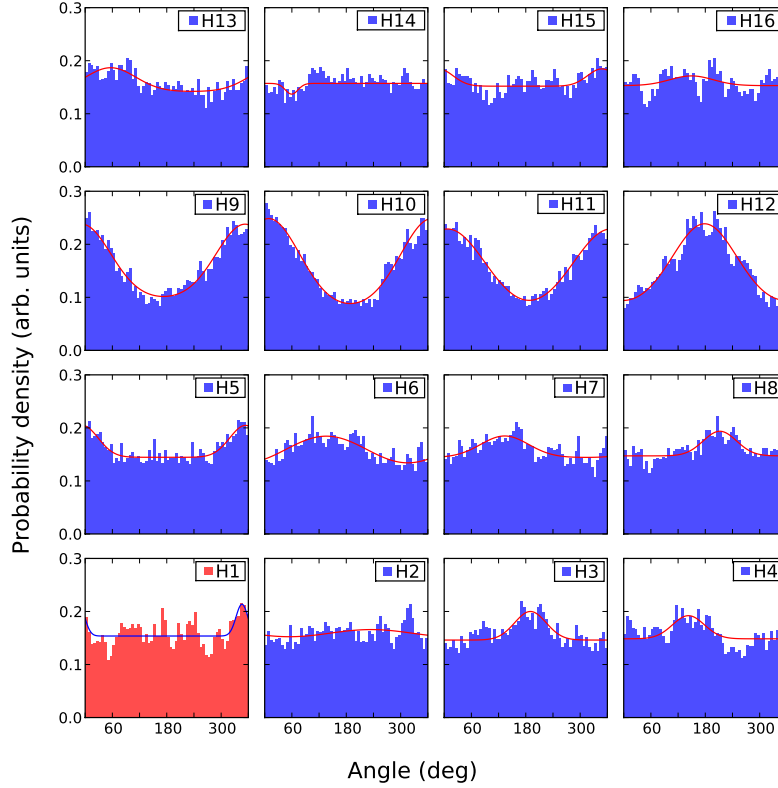


Figure 8. Relative angular distribution of hydrogen atoms in the $2 \times 2 \times 2$ supercell. The results are obtained from a 18 ps MD run at 150 K. Solid line shows the function $\mathcal{F}_\sigma(\varphi)$ given by equation (3) fitted to the data. Positions of hydrogen atoms with labels H1, H2, ..., H16 are shown in figure 1.

disappear for different atoms.

For higher temperatures, above 30-40 K, the absolute angular positions of hydrogen atoms are completely decoupled from the directions of crystal lattice (figure 6) but we can still observe fairly strong correlations in relative angular positions of hydrogen atoms — these correlations are robust and persist even in the regime of rather high temperature. Figure 8, obtained for temperature $T = 150$ K, presents an essentially unchanged picture of the distribution of hydrogen atoms' relative positions. One can notice that weaker correlations with atoms from the first and from the last row seem to have disappeared. However, this may be due to the smaller statistics of the sample (18 ps vs. 39 ps) and higher noise in the data obtained for this case.

4.2. Angular distribution of hydrogen positions

We have constructed a simple probabilistic model to describe measured angular distribution of hydrogen atoms. As a starting point it is reasonable to assume a Gaussian distribution around one location accompanied by a constant background filling for the rest of the histogram. In periodic angular coordinates the standard

Gaussian distribution in angle φ centred at μ with width σ ,

$$\mathcal{P}_\sigma(\varphi) = \frac{1}{\sigma\sqrt{2\pi}} \exp\left[-\frac{(\varphi - \mu)^2}{2\sigma^2}\right], \quad (1)$$

should be summed up over periodic repetitions of itself, which leads to

$$\frac{1}{\sigma\sqrt{2\pi}} \sum_{k=-\infty}^{\infty} \exp\left[-\frac{(\varphi - \mu + 2\pi k)^2}{2\sigma^2}\right] = \frac{1}{2\pi} \vartheta_3\left(\frac{\varphi - \mu}{2}, e^{-\frac{\sigma^2}{2}}\right). \quad (2)$$

Here ϑ_3 is an elliptic Jacobi function of the third kind. Thus, the angular distribution we introduce here reads:

$$\mathcal{F}_\sigma(\varphi) = \mathcal{N} \left[(1 - \alpha) \frac{1}{2\pi} \vartheta_3\left(\frac{\varphi - \mu}{2}, e^{-\frac{\sigma^2}{2}}\right) + \alpha \right], \quad (3)$$

where \mathcal{N} is a normalizing factor. It consists of the correlated part given by equation (2) with intensity $(1 - \alpha)$ and the background with intensity α .

One can notice that in the case of 30 K (figure 7) as well as for 150 K (figure 8) the model for the angular distribution given by equation (3) fits the obtained numerical data remarkably well — it indicates the existence of a single potential minimum in relative motion of individual hydrogen atoms. This demonstrates that relative angular distribution reflects the correlated behavior of the hydrogen atoms, with a single optimal angular position for each hydrogen atom. This is obviously not the case in the absolute angular positions depicted in figure 5, where a two-peaked distribution would be required to describe the data.

We should also note that the atoms $\{H_9, H_{10}, H_{11}, H_{12}\}$ are characterized by strongly correlated movement with respect to the atom H_1 . They are located in the same structure layer as the reference (H_1) atom. Also the position of a single out-of-plane atom H_5 , located directly above the reference atom H_1 on the same three-fold axis, is strongly correlated with that of atom H_1 . Moreover, it is clear that the directions of the peaks do not strongly follow 60° grid present in the smaller unit cell. The strongest signal indicates same/opposite direction arrangement of the direct neighbour (atom H_9) of the reference atom and its images in the neighbouring unit cells (H_{10} - H_{12}). However, if we look closer at the distributions presented in figure 7, we can notice small preference for image atoms (H_2 - H_4) to cluster around 120° and 240° directions. This result does not offer strong support for the XGT/XLT arrangement hypothesis but the preferred directions are compatible with this type of arrangement.

In light of these results we conclude that the angular correlations in the atomic distribution obtained for the small unit cell is likely just an artefact of the constraints imposed on the system by the $\sqrt{3} \times \sqrt{3} \times 1$ unit cell. We also believe that it is still possible that the real physical system exhibits one of the symmetries proposed before [9, 7, 13, 16, 17, 18], but we emphasize that it does not show these symmetries for system size up to the $2 \times 2 \times 2$ supercell.

5. Summary and Conclusions

We have performed extensive calculations to determine the structure and elastic properties of magnesium hydroxide. The static calculations confirm the main result of the previous research that static average structure with hydrogen atoms on the three-fold axis is absent in the brucite crystal. Further static calculations of the elastic constants of brucite also support conclusions from previous papers [9, 7, 13, 17, 18, 19]

suggesting existence of the superstructure, probably with the $P\bar{3}$ symmetry, and XGT arrangement of the hydrogen atoms [13]. This, however, does not exclude all other possibilities which would be still consistent with the available experimental evidence.

In the present paper we have investigated one of such possibilities — existence of hydrogen sublattice possibly almost decoupled from the rest of the crystal. The results from the MD calculations in the small supercell support this hypothesis. Furthermore, the calculations performed in the larger $2\times 2\times 2$ cell revealed correlations between neighbouring hydrogen atoms at temperature between 30 K and 150 K. We have not found any lock-in behaviour of the hydrogen system above $T = 30$ K, while below this temperature we have identified strong correlations between angular positions of hydrogen atoms and orientation of the lattice vectors. This result indicates that the rotational (around the three-fold axis) degree of freedom of hydrogen system gets decoupled from the crystal lattice around temperature $T = 30$ K which may be considered as a characteristic energy scale for the onset of hydrogen-lattice coupling.

The $2\times 2\times 2$ supercell (shown in figure 1) is the largest one available for practical use at the moment, and additional calculations of lattice dynamics performed for the $3\times 3\times 3$ supercell indicate that the long-range interactions do not modify lattice dynamics in any significant way. Thus, we expect that the main qualitative conclusions on the crystal symmetry and hydrogen angular correlations either would not change, or would even strengthen in a larger system, when technology and algorithms will develop to the point that larger systems could be investigated.

The results presented above demonstrate that the angular coordinates of the hydrogen atoms in the brucite crystal are likely decoupled from the crystal lattice above the estimated characteristic temperature $T \simeq 30$ K. We have provided evidence that, in spite of this partial disorder in the hydrogen subsystem, angular correlations between positions of hydrogen atoms are robust and survive also in the high temperature regime $T \simeq 150$ K. We believe that these results will stimulate further research and the issue of inter-hydrogen correlations in brucite and related crystals should be further investigated using theoretical as well as experimental methods. We suggest that nuclear magnetic resonance spectroscopy could be a useful experimental tool in this context.

Acknowledgments

This work was partially supported by Marie Curie Research and Training Network under Contract No. MRTN-CT-2006-035957 (c2c) and Polish Ministry of Science and Education Grant No. 541/6.PR UE/2008/7. A M Oleś acknowledges support by the Foundation for Polish Science (FNP).

References

- [1] Finger L W and Prewitt C T 1989 *Geophysical Research Letters* **16** 1395–1397
- [2] Kanzaki M 1991 *Physics of The Earth and Planetary Interiors* **66** 307
- [3] Kruger M B 1989 *Journal of Chemical Physics* **91** 5910
- [4] Duffy T S, Ahrens T J and Lange M A 1991 *Journal of Geophysical Research* **96** 14319
- [5] Redfern S A T and Wood B J 1992 *American Mineralogist* **77** 1129–1132
- [6] Fei Y and Mao H K 1993 *Journal of Geophysical Research* **98** 11875
- [7] Catti M, Ferraris G, Hull S and Pavese A 1995 *Physics and Chemistry of Minerals* **22** 200–206
- [8] Duffy T S, Meade C, Fei Y, Mao H K and Hemley R J 1995 *American Mineralogist* **80** 222–230
- [9] Parise J B, Leinenweber K, Weidner D J, Tan K and Von Dreele R B 1994 *American Mineralogist* **79** 193–196

- [10] Sherman D M 1991 *American Mineralogist* **76** 1769–1772
- [11] D’Arco P, Causà M, Roetti C and Silvi B 1993 *Phys. Rev. B* **47** 3522–3529
- [12] Raugai S, Silvestrelli P L and Parrinello M 1999 *Phys. Rev. Lett.* **83** 2222–2225
- [13] Mookherjee M and Stixrude L 2006 *American Mineralogist* **91** 127–134
- [14] Zigan F and Rothbauer R 1967 *Neues Jahrbuch für Mineralogie Monatshefte* 137–143
- [15] Partin D E, O’Keefe M and Von Dreele R B 1994 *Journal of Applied Crystallography* **27** 581–584
- [16] Megaw H 1973 *Crystal Structures: A Working Approach*. (W.B. Sanders Company, Philadelphia.)
- [17] Parise J B, Theroux B, Li R, Loveday J S, Marshall W G and Klotz S 1998 *Physics and Chemistry of Minerals* **25** 130–137
- [18] Parise J B, Loveday J S, Nelmes R J and Kagi H 1999 *Phys. Rev. Lett.* **83** 328–331
- [19] Desgranges L, Calvarin G and Chevrier G 1996 *Acta Crystallographica Section B: Structural Science* **52** 82
- [20] Kresse G and Furthmüller J 1996 *Computational Materials Science* **6** 15–50 ISSN 0927-0256
- [21] Kresse G and Joubert D 1999 *Phys. Rev. B* **59** 1758–1775
- [22] Perdew J P, Burke K and Ernzerhof M 1997 *Phys. Rev. Lett.* **78** 1396
- [23] Blchl P E 1994 *Phys. Rev. B* **50** 17953–17979
- [24] Monkhorst H J and Pack J D 1976 *Phys. Rev. B* **13** 5188–5192
- [25] Jochym P, Parlinski K and Sternik M 1999 *European Physical Journal B: Condensed Matter and Complex Systems* **10** 9–13
- [26] Jochym P and Parlinski K 2000 *European Physical Journal B: Condensed Matter and Complex Systems* **15** 265–268
- [27] Nos S 1984 *Journal of Computational Physics* **81** 511–519
- [28] Parlinski K, Li Z Q and Kawazoe Y 1997 *Phys. Rev. Lett.* **78** 4063–4066
- [29] Parlinski K 2005 PHONON, lattice dynamics software
- [30] Jiang F, Speziale S and Duffy T S 2006 *American Mineralogist* **91** 1893–1900